Nonlinear Analysis and Experimental Results of Doubly Salient PM Generator

Bülent Şarlıoğlu
Honeywell International
Electro-Mechanical Power Systems
2525 W. 190th St. Torrance, CA 90504
bulent@ieee.org

Thomas A. Lipo
University of Wisconsin - Madison
Electrical and Computer Engineering Department
1415 Engineering Dr. Madison, WI 53706
lipo@engr.wisc.edu

Abstract – **In this paper, nonlinear modeling, simulation and experimental results are presented for the doubly salient permanent magnet (DSPM) generator. Due to the highly nonlinear magnetic structure of the DSPM generator, the utilization of first order approximations for back emf and inductance profiles does not provide high accuracy. Nonlinear analysis obtained from the finite element analysis are further extended by using cubic splines to obtain the instantaneous back emf and inductance characteristics. These results are incorporated into the dynamic simulation of the DSPM machine and power electronic converter together. The accuracy of the nonlinear analysis are verified with both static and dynamic experimental results. Also in this paper, the utilization of ac output of the DSPM generator has been presented**

1. INTRODUCTION

The improvements in permanent magnets and power electronics technologies have made it possible to devise different configurations of electrical machines which were not previously possible to implement. For this purpose, the Doubly Salient Permanent Magnet (DSPM) AC machines [1-6, 14, 15, 16], in which the field is excited by either stationary or rotating high density permanent magnets, have been developed in University of Wisconsin-Madison.

The generator version of the DSPM machine investigated has four stator poles and six rotor poles as illustrated in Fig. 1. Two Neodymium Iron Boron permanent magnets are located in the stator yoke. Since there are no windings or permanent magnets in the rotor, the DSPM generator has several advantages: the rotor has low inertia, no copper loss, no PM attachments, no brushes, and no slip rings. This type of rotor can be manufactured easily, and can be run at very high speeds as in the case of a switched reluctance machine. Fig. 2 depicts the inductance and flux linkage with respect to the rotor position using first order approximations.

Compared to induction and switched reluctance machines, the DSPM generator can produce more power from the same geometry [2], [16]. Moreover, the efficiency of the DSPM generator is higher, since there is no copper loss associated with excitation of the machine. Another advantage of the DSPM generator is that the output AC voltage can easily be rectified by a diode bridge rectifier, while in the case of the switched reluctance machine one needs to use active semiconductor switches for power generation. If greater utilization and control of power production capability are desired, the AC output of the DSPM generator can be rectified using an active converter. Consequently, this new type of generator is a promising candidate for power generation where the efficiency, weight, and volume of the generator are important concerns.

The design of machines with a doubly salient structure with conventional approaches is not sufficiently accurate due to the many assumptions required. For example,

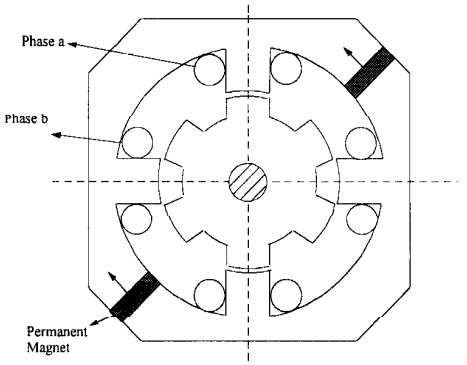

Fig. 1 A typical lamination for 4/6 DSPM Generator

assumptions made in conventional magnetic design include neglecting or simplification of the saturation effect of the iron, fringing at the non-overlapping stator and rotor pole tips, inner and outer leakage flux of the permanent magnets, and uneven distribution of the flux density. While conventional magnetic circuit design may be sufficient for an initial estimation of parameters for the DSPM machine, early designs have shown the need for refining the accuracy of the design method. However, it is more important to use these results gainfully to understand the behavior of this machine with power electronic circuitry, since the design goal is an optimized match for the performance of the machine and power electronics circuitry together, as in the case of a SRM drive.

There has been various contributions for demonstration the capabilities and magnetic nature of the DSPM machine topologies. The first contribution has been to modify the design method and evaluate the pitfalls of the analytical design by taking into account nonlinear results obtained from FEM analysis. The second contribution is to use FEM results to acquire flux vs. current data for different rotor positions for use in a *dynamic simulation*, which is less often reported in the literature [7-11].

Various attempts have been made to model the flux linkage/current/rotor position relationship. Piecewise first- or second-order functions of flux linkage with respect to rotor position, with current as an undetermined parameter, are used for a rapid SRM computer algorithm in reference [7]. A quasi-linear model for an SRM was presented in reference [10] in which two lines are used to represent saturated and unsaturated portions of the flux linkage/current curves. In reference [11], authors solve the voltage equations by using an input table $i(\lambda,\phi)$, and intermediate values of $i(\lambda,\phi)$ required in the integration of the voltage equation are obtained by linear interpolation in rotor angle and quadratic interpolation in flux linkage instead of partial derivatives of the flux linkage.

Since dynamic modeling for simulating the machine and power electronic circuitry together requires the partial derivative of the flux with respect to current where rotor position is a parameter, and the partial derivative of the

flux with respect to rotor position where the current is a parameter, interpolation of these resulting curves is critical. It is shown in this paper that such interpolation can be achieved via cubic or B-splines. These results are used for a more accurate dynamic simulation of the machine and power electronics circuitry and are verified with experimental results. Finally, the utilization of ac output of the DSPM generator has also been presented in this paper.

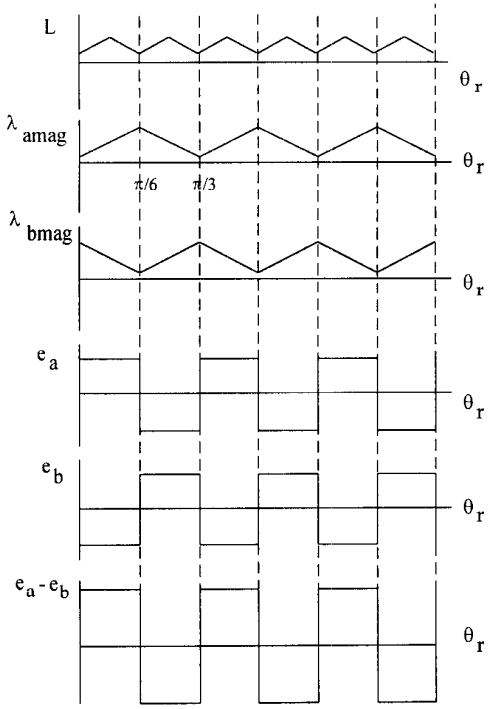

Fig. 2 The phase inductance and permanent magnet flux variations with respect to rotor position. From top to bottom: L - inductance of phases a and b, λ_{amag}, λ_{bmag} - magnet flux linking a and b phases, E_a-E_b - emfs induced in a and b windings, e_a-e_b –emf if windings are connected in series. (π/6 – full alignment, π/3 full misalignment.)

2. FINITE ELEMENT ANALYSIS OF DSPM GENERATOR

Detailed studies of the magnetic flux linkage of the DSPM generator as a function of rotor position and current in the windings have been carried out using the finite element method as utilized in the SRM machines, and the discrete results are shown in circles in Fig. 3. The details of FEM analysis can be found in reference [2], [14], and [16]. In Fig. 4, a different representation of the same data in Fig. 4 is given by changing the parameter to phase current.

The full-alignment of the rotor is assumed to occur at 0 degrees while the full-misalignment occurs at 30 degrees (when the rotor tooth leaves the stator tooth) or -30 degrees (when the rotor tooth comes into alignment with the stator tooth).

3. CUBIC SPLINE THEORY AND ITS APPLICATION TO DOUBLY-SALIENT MACHINES

The above analysis of the DSPM generator and its waveforms shown in Fig. 2 are based on the first order approximations. The emf induced in the winding can be found by taking the derivative of the flux linking that coil with respect to time. Mathematically, for a given phase

$$e = \frac{d\lambda}{dt} = \frac{\partial\lambda(\theta,i)}{\partial\theta}\frac{d\theta}{dt} + \frac{\partial\lambda(\theta,i)}{\partial i}\frac{di}{dt} \qquad (1)$$

$$e = BEMF(\theta,i)\frac{d\theta}{dt} + L(\theta,i)\frac{di}{dt} \qquad (2)$$

For dynamic simulation, two partial derivatives, one of flux linkage with respect to rotor position and the other with respect to current are needed.

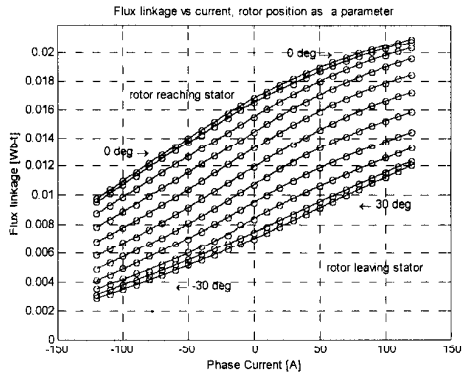

Fig. 3 FEM results showing flux linkage vs. current and rotor position is a parameter for a pole winding.

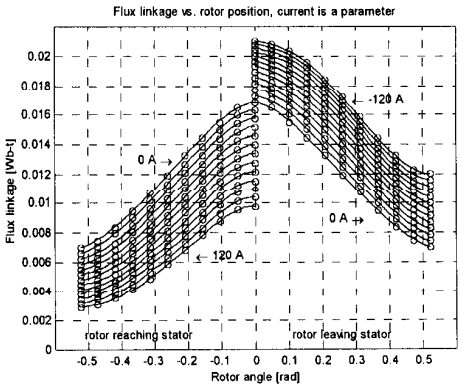

Fig. 4 Flux linkage vs. rotor angle for a pole winding for various current levels.

To achieve this goal, cubic splines can be used in which cubic polynomials are utilized to connect data points where the resulting spline function has two continuous derivatives everywhere [12], [13]. Moreover, every individual cubic function is then connected at each data point (also called knot) forming a smooth curve. For a particular rotor position, if there are n points of data for a flux linkage λ, then the spline function λ(i) will have n-1 cubic polynomials:

$$\lambda_k(i) = a_k(i - i_k)^3 + b_k(i - i_k)^2 + c_k(i - i_k) + d_k \qquad (3)$$

where i is the instantaneous phase current at the interval of $i_k < i < i_{k+1}$ and subscript k is k = 1,2, ..., n-1. Fig. 5 depicts the application of spline theory to a λ versus i data set curve.

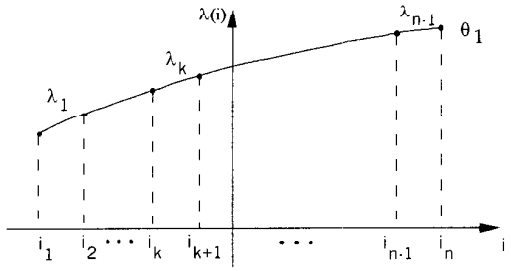

Fig. 5 Illustration of spline theory for flux linkage vs. current for a specific rotor position

Four parameters a_k, b_k, c_k, and d_k need to be determined for every segment. This can be done by evaluating four conditions for each segment.

$$\lambda_k (i_k) = d_k \qquad (4)$$

$$\lambda_k(i_{k+1}) = a_k(i_{k+1} - i_k)^3 + b_k (i_{k+1} - i_k)^2 + c_k (i_{k+1} - i_k) + d_k \qquad (5)$$

$$\frac{d\,\lambda_{k+1}(i_{k+1})}{di} = \frac{d\,\lambda_k(i_{k+1})}{di} \qquad \frac{d\,\lambda^2_{k+1}(i_{k+1})}{di^2} = \frac{d\,\lambda^2_k(i_{k+1})}{di^2} \qquad (6)$$

A boundary condition is also needed for the solution. Mathematical algorithms are available to find the four unknown parameters for each segment and can be implemented in computer code. In the study being reported, the MATLAB spline toolbox was used. Detailed procedure is given in reference [14].

Results for the partial derivatives $\frac{\partial\lambda(\theta,i)}{\partial\theta}$ and $\frac{\partial\lambda(\theta,i)}{\partial i}$ of a winding are obtained by taking the derivative of spline functions developed and are shown in Fig. 6 and Fig. 7. These figures enable the analyst to visualize what is happening to instantaneous generated voltage and inductance as the phase current and rotor position are changed.

4. EXPERIMENTAL STATIC TESTING OF THE DSPM GENERATOR

Using the analysis methods described a prototype DSPM generator has been designed, built and tested to evaluate its performance. The purpose of the static testing of the prototype generator is to obtain the flux linkage with respect to the current value or the instantaneous inductance with rotor position as a parameter. In this test, rotor is locked at discrete rotor positions. A sinusoidal voltage is applied to the machine where the two phase windings are connected in series. For each rotor position, the sinusoidal voltage is increased until 120 A peak current is achieved. Current and voltage waveforms across one phase are sensed and stored in a disk from an oscilloscope. Using the Faraday's law flux linkage at different positions can be obtained as

$$\lambda = \int_0^t (v - R\,i)\,dt + \lambda_{0f} \qquad (7)$$

where v is the instantaneous voltage across the phase, R is the phase resistance, i is the instantaneous phase current, and λ_0 is the initial value of the flux linkage.

Fig. 8 shows the results for the flux linkage versus current for three important rotor positions by making the assumption that the prototype generator has the same permanent magnet flux linkage as that of the finite element analysis. Since the slope of these curves at any instant is the incremental inductance of the generator, the inductance values obtained from the testing are in good correlation with those obtained from the finite element analysis. These overlaid plots convincingly suggest that the nonlinearity of the DSPM machine can be predicted by using tools such as nonlinear finite element analysis.

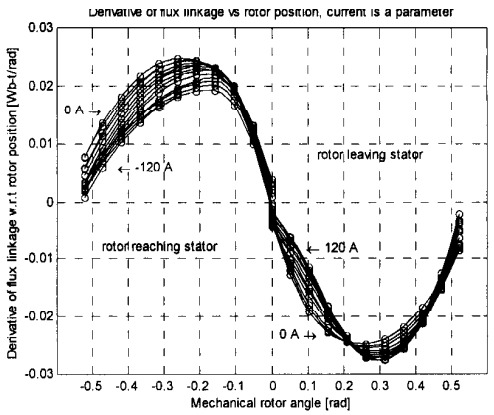

Fig. 6 The partial derivative of pole flux linkage with respect to rotor position, i.e. $\frac{\partial\lambda(\theta,i)}{\partial\theta}$ (current is a parameter).

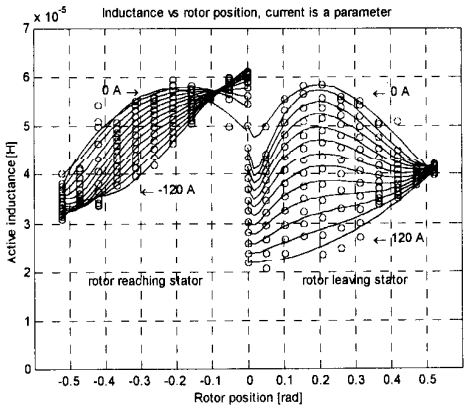

Fig. 7 The partial derivative of pole flux linkage with respect to phase current, i.e. $\frac{\partial\lambda(\theta,i)}{\partial i}$ for incremental rotor positions.

5. NO-LOAD ROTATIONAL TESTING

This test aims to obtain the flux linkage with respect to position or back emf voltage. A separately-excited dc motor is used as a prime mover to run the DSPM generator at various speeds. Individual voltages of the two phases and the sum of the voltages of the two phases are measured. To assess the accuracy of our finite element modeling and cubic spline modeling with respect to actual machine performance, the back emf voltages obtained from FEM analysis and experimental data at 3000 rpm are overlaid as shown in Fig. 9. It is observed that experimental data is in good correlation with the predicted results.

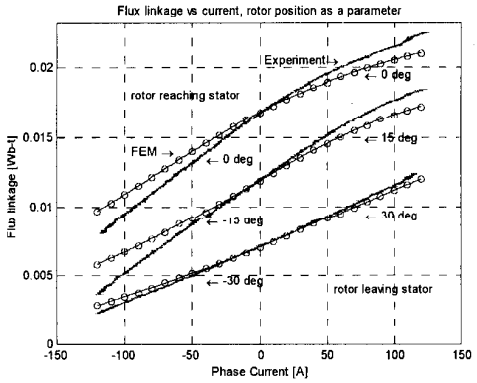

Fig. 8 Flux Linkage vs. Current for aligned (0 deg), half-aligned (15 deg), and full-misaligned (30 deg) positions. Straight curves are from experimental results: circled data points are from finite elements.

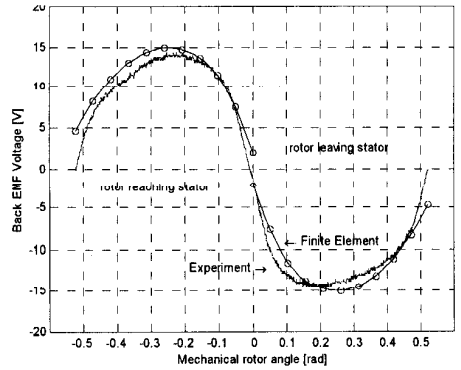

Fig. 9 Comparison of Experimental results vs. FEM: No-load back emf of one phase at 3000 rpm.

6. EXPERIMENTAL RESULTS AND NONLINEAR SIMULATION

A- Bridge Rectifier with Constant DC Link Current

The ac voltage output of the DSPM generator can easily be rectified to obtain a dc voltage. As a case study, a bridge rectifier is used for this purpose, assuming that the dc link current is essentially constant due to a large dc link inductor as shown in Fig. 10. Waveforms obtained from the experiment are shown in Fig. 11. The generator is run at 3000 rpm and the dc link current loading is 30.8 A.

A simulation is also done using the nonlinear results obtained to verify the accuracy of the modeling. By using the sink convention ($i = -i_{ac}$), the stator current is

$$\frac{di}{dt} = \frac{\pm V_{dc} - (R_a + R_b)\, i - (BEMF_a(\theta,i) + BEMF_b(\theta,i))\frac{d\theta}{dt}}{L_a(\theta,i) + L_b(\theta,i)} \quad (8)$$

where results for partial derivatives $BEMF_x(\theta,i)$ and $L_x(\theta,i)$ for each phase are found by iteration from the look-up table stored in the simulation. Diode voltage drops (3.5 V) are also included in the simulation. Stator current is obtained by simulating eqn.8 and results are shown in Fig. 12. In this simulation, the dc link current and rotor speed are set to same as those of the experiment.

DC output power is calculated as 384 W experimental, while it is 425W from the simulation. The difference is at 10 %. Also, the commutation times of current from the experiment and simulation are 610 μs and 700 μs, respectively. Therefore, a good correlation is also achieved in this portion of the waveform.

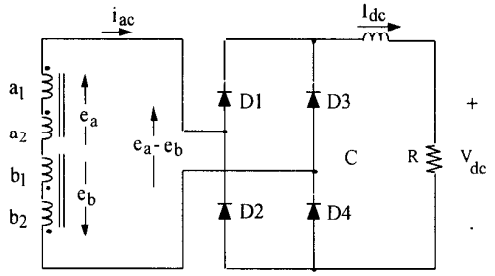

Fig. 10 Rectification with constant dc current.

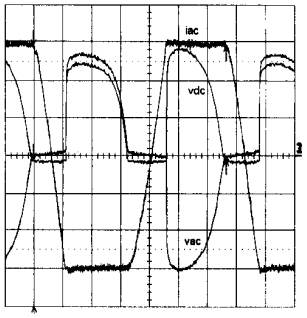

Fig. 11 Experimental results: (Traces: Voltages 10 V/div, current 20 A/div)

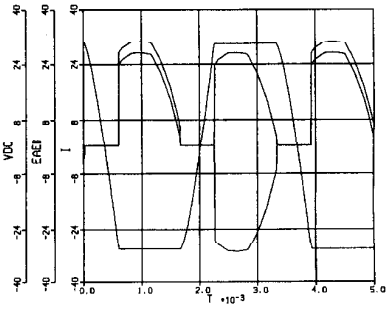

Fig. 12 Simulation results: Rectified voltage, voltage e_a-e_b and current i ($i = -i_{ac}$).

Fig. 13 illustrates other important quantities for the same simulation. It can be noted that waveforms of the inductance and the back emf of the machine are much different than using the first approximation shown in Fig. 2. For example, the inductance values obtained from the conventional analysis are one and half to two times less than those obtained from nonlinear analysis. The dc power output and commutation time using first order approximations are calculated 664 W and 409 μs, respectively. Considering the dc power output and commutation time from experimental results were 384 W and 700 μs respectively, the results are not as accurate as it has been obtained from the nonlinear analysis. Therefore, the prediction of overall performance calculation can be done more realistically by using nonlinear modeling, since both inductance and back emf terms determine the commutation period, and hence power transfer from the ac generator output to the dc load.

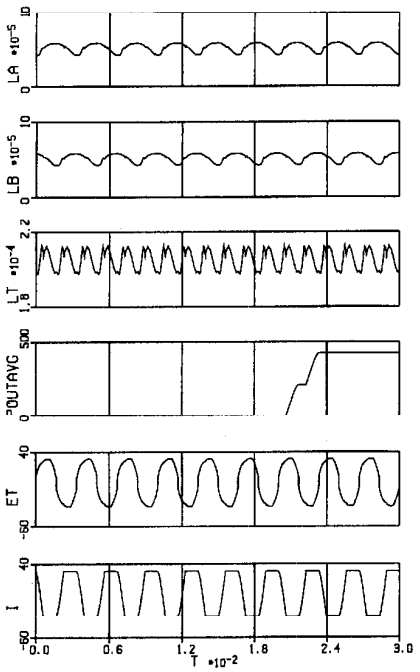

Fig. 13 Nonlinear simulation results: (Top to bottom: Phase a and b inductance, total inductance L_t, average dc output power P_{outavg}, back emf voltage (BEMF) E_t, and current I.)

B. Bridge Rectifier with Constant DC Link Voltage

This is a similar test to that in the previous section, except the output voltage of the bridge rectifier is kept constant by a sufficiently large capacitor. The capacitor is connected in parallel with the load. Fig. 14 depicts the waveforms obtained at 3000 rpm with C_{dc} = 20 mF and R_{dc} = 0.75 ohm.

The power output have been obtained 1400 W, 1320 W, and 1710 W from experiment, nonlinear simulation, and first order approximation simulation. Therefore, the first order approximation simulation overestimates the power production capability by 20 percent due to the simplified inductance and back emf voltage modeling. However, nonlinear simulation provides better accuracy as in the case of rectifier with constant dc link current.

C. BOOST CONVERTER WITH HYSTERESIS CURRENT CONTROLLER

The ac output of the DSPM generator is rectified by a boost converter with a hysteresis current controller as shown in Fig 15. A hysteresis controller is designed and built for this purpose. A variable current reference was generated from the signals obtained from the position sensors.

Fig. 16 shows the low speed results at 870 rpm. The generator current is controlled by using a reference. It can be observed that the AC voltage is not zero when the machine is short-circuited due to the diode and IGBT voltage drops. From Fig. 16-right, the output voltage has considerable ripple, since the output capacitor is not sufficiently large. In this case, the output capacitance is 20 mF, paralleled with the load for filtering the dc output voltage.

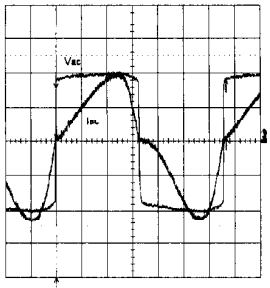

Fig. 14 AC output voltage (10 V/div) and AC output current (20A/div) of the DSPM generator

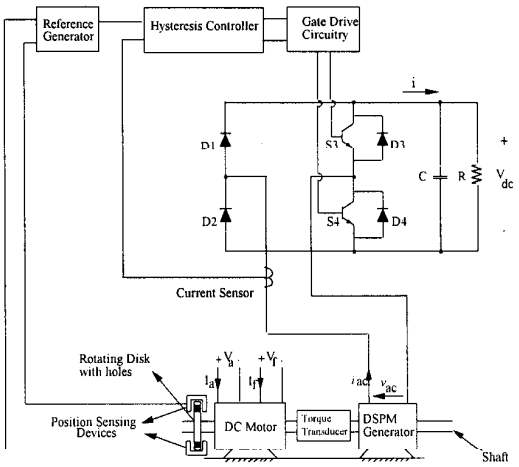

Fig. 15 Schematics of implementation of the boost converter with hysteresis current controller

Results at 3000 rpm are illustrated in Fig. 17. The bottom trace of Fig. 17-left shows the reference current and actual current. It can be seen that the measured current tracks the reference current very well. The rise of the actual current to the reference current is slower than when the actual current goes to zero. This is mainly due to the operation principle of the boost converter. The machine back emf is applied to the machine inductance when one diode and one IGBT are on. A larger voltage, which is the sum of the back emf and the dc output voltage, is applied to the generator inductance, when the two diodes are on and the generator is connected to the load short. As can be seen from Fig. 17-right the output voltage no longer has much ripple, since the output capacitor is increased to 64 mF from 20 mF. The switching frequency in this case is measured as 2.4 kHz.

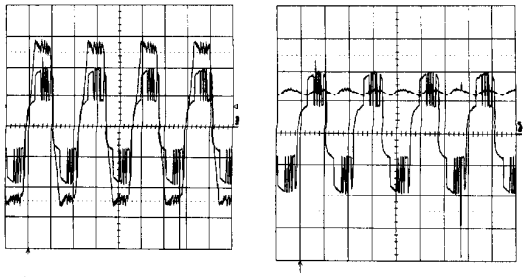

Fig. 16 Left: AC current (10 A/div) and AC voltage (4.85 V/div) at 870 RPM Right: DC voltage (5 V/div) and AC voltage (4.85 V/div) at 870 RPM

The dc output voltage is measured at 35 V and power at the dc side is calculated as 612.5 W when the load is 2 ohms at the output. Considering the diode and IGBT drops, the ac power is more than the dc power. If it is noted that the output power of the rectifier with constant dc output voltage at 2 ohms is 220 W, using the boost converter with a hysteresis controller can increase the output power by a factor of two and three quarters (2.75). This is mainly due to the fact that the output power can be maximized by choosing the optimum current reference. Also the reference can be advanced to attempt to make the voltage and current in phase. From this it can be concluded that a better utilization of the DSPM generator can be obtained by using actively controlled power electronics topologies rather than passive ones. However, the cost and complexity of the controlled power conversion are greater.

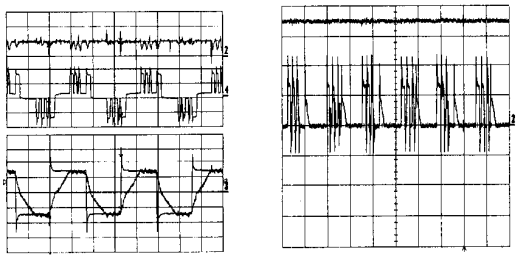

Fig. 17 3000 RPM , Torque 150 inch-lbs/V, AC voltage (25 V/div) (moved down by 1.8 divisions for clarity of illustration), Current reference (50A/div), Current (50A/div) Left: DC voltage (10 V/div) and DC current (50 A/div)

7. CONCLUSION

In this paper, it is demonstrated that nonlinear analysis obtained from finite element analysis can be further extended by using cubic splines to enable the analyst to readily simulate the machine and power electronic converter together. By using this method the instantaneous back emf and inductance terms can be better visualized and also utilized to predict the design and performance goals of the generator. The accuracy of the proposed approach are compared with experimental results and a good correlation is achieved. It should be noted that the proposed approach can be used for other highly nonlinear machines for which generalized machine theory and lumped-parameter modeling either do not exist or fail to give accurate results.

Also in this paper, the utilization of ac output of the DSPM generator has been presented. Rectifiers with constant dc voltage and constant dc current can be used for transferring ac power of the DSPM generator to dc power for inexpensive and simple power conversion. Also, a boost converter with hysteresis controller is designed for converting ac to dc power. In this case, complexity and cost are increased. However, more power output is obtained by using a boost converter than using diode bridge rectifiers due to the active control of the magnitude and phase of the current reference.

8. ACKNOWLEDGEMENT

Wisconsin Electrical Machine and Power Electronics Consortium (WEMPEC) at University of Wisconsin-Madison is gratefully acknowledged for funding this project. Thanks is also given to Miller Electric Company (Milwaukee, Wisconsin) for construction of the generator.

REFERENCES

[1] Sarlioglu, B., Zhao, Y., Lipo, T.A., "A Novel Doubly Salient Single Phase Permanent Generator", *IEEE IAS Annual Meeting*, Denver, CO, Oct. 2-6, 1994, pp. 9-15.

[2] Sarlioglu, B., Lipo, T.A., "Comparison of Power Production Capability Between Doubly Salient Permanent Magnet and Variable Reluctance Type Generators", 1995 Aegean Conference on Electrical Machines and Power Electronics, Kusadasi, Turkey, June, 1995.

[3] Lipo, T.A., Li, Y., Luo, X., Sarlioglu, B., "Doubly Salient Permanent Magnet Machines- A Progress Report", International Symposium on Electric Power Engineering, Stockholm, June 18-22, 1995.

[4] Liao, Y., Liang, F., and Lipo, T.A., "A Novel Permanent Magnet Motor with Doubly Salient Structure", *IEEE IAS Annual Meeting*, Houston TX, Oct. 5-8, 1992, pp. 308-314.

[5] Shakal, A., Liao, Y., Lipo, T.A., " A New Permanent Magnet Motor Structure with True Field Weakening", IEEE International Symposium on Industrial Electronics, Budapest, Hungary, June 1993, pp. 19-24.

[6] Liao, Y. and Lipo, T.A., "Sizing and Optimal Design of Doubly Salient Permanent Magnet Motors", IEE 6th International Conference on Electrical Machines and Drives, Sept. 8-10, 1993, pp. 452-456.

[7] Miller, T. J. E., and McGlip, M., "Nonlinear Theory of Switched Reluctance Motor for Rapid Computer-Aided Design", IEE Proceedings, Vol 137, Pt. B, No.6, November, 1990.

[8] Moallem, M.and Ong, C.M., "Predicting the Torque of a Switched Reluctance Machine From its Finite Element Solution", *IEEE Transactions Energy Conversion*, Vol.5, No.4, December 1990.

[9] Miller, T.J.E, "Converter Volt-Ampere Requirements of the Switched reluctance Motor Drive", IEEE-IAS Annual Meeting, Chicago, IL, October, 1984.

[10] Ray, W.F., Lawrenson, P. J., Davis, R.M, Stephenson, J.M., Fulton, N.N., and Blake, R.J., "High-Performance Switched Reluctance Brushless Drives", IEEE-Transactions on Industry Applications, Vol. IA-22, No.4, July/August 1986.

[11] Stephenson, J.M. and Corda, J., "Computation of Torque and Current in Doubly Salient Reluctance Motors from Non-linear Magnetisation data", Proc. Inst. Elec. Eng., vol. 126, pp. 393-396, May 1979.

[12] Borse, G.J, Numerical methods with MATLAB : *A Resource for Scientists and Engineers*, PWS Publishing, 1997.

[13] Burden, L.B. and Faires, J.D., *Numerical Analysis*, PWS Publishing company, 1993.

[14] Sarlioglu, B. and Lipo, T.A., "Nonlinear Modeling and Simulation of Single Phase Doubly Salient Permanent Magnet Generator", *IEEE IAS Annual Meeting*, St. Louis, MO, Oct. 12-15, 1998.

[15] Sarlioglu B. and Lipo T.A., "Assessment of Power Generation Capability of Doubly Salient PM Generator", *IEEE-International Electric Machines and Drive Conference*, May 9-12, Seattle, Washington, 1999

[16] Sarlioglu B., "Design and Analysis of a Novel Doubly-Salient Permanent Magnet Generator", Ph.D. Dissertation, Electrical Engineering, University of Wisconsin-Madison, Madison, Wisconsin, 1999